Stress-Oriented Structural Optimization for Frame Structures

Abstract

To fabricate a virtual shape into the real world, the physical strength of the shape is an important consideration. We introduce a framework to consider both the strength and complexity of 3D frame structures. The key to the framework is a stress-oriented analysis and a semi-continuous condition in the shape representation that can both strengthen and simplify a structure at the same time. We formulate a novel semi-continuous optimization and present an elegant method to solve this optimization. We demonstrate our approach with applications such as topology simplification and structural strengthening.

Keywords: 3D printing, fabrication, stress analysis, optimization, topology simplification

1 Introduction

We have witnessed many developments in the area of computational fabrication in recent years [1, 2, 3, 4]. As 3D printers become increasingly common and affordable, there is a great need for tools that consider the physical properties of virtual meshes. When bringing virtual objects into the real world through 3D printing, the strength of an object is one such important consideration. We present a framework to analyze both the strength and complexity of 3D frame structures, where a structure consists of a set of beams. The motivations for focusing on frame structures are that these structures are common in architectural models, they can also represent general 3D shapes, and they can be 3D printed as a real-world frame structure to represent the virtual shape without an excessive amount of printing material.

There has been some recent work exploring the idea of strength analysis of 3D printed shapes [5, 6, 7]. There also exists work that analyze structural parts and reduce the cost of 3D printing by building a skin-frame structure [8] or a honeycomb-cells structure [9]. In this paper, we introduce a single stress-oriented framework to analyze the strength and complexity of 3D frame structures at the same time. A key contribution different from previous work is that we have a problem formulation and a semi-continuous condition in our shape representation. This condition can remove structurally redundant elements to reduce the overall shape complexity without sacrificing its structural strength.

We formulate our problem to optimize scalar parameters of a frame structure such that it is 3D printable with high strength, while taking into account the volume, symmetric, semi-continuous, and sparsity constraints. These constraints are quite intuitive, as they limit the size and complexity of the output structure while maintaining its aesthetics. The idea is to strengthen weak parts while maintaining the overall volume of the shape, and optionally changing the topology and maintaining the shape symmetry. In particular, the semi-continuous constraint is key to our formulation, as it includes a choice between lower and upper bounds and a value of zero for each parameter in the shape representation. An element within a shape with a parameter value of zero will disappear. Our formulation of this condition in the problem allows us to explore the tradeoffs between strength and complexity in frame structures. The user can also control the tradeoff to choose among structures with various simplified topologies and high strength.

We use stress as a measure of strength of an object. We consider the frame structure as a set of beam elements and compute the stress of each element. Our stress-oriented structural optimization then minimizes the maximal stress of all elements. The semi-continuous condition in our shape representation requires a non-trivial solution to this problem. Hence we formulate a novel semi-continuous optimization and present an elegant method, the alternation direction method of multipliers (ADMM) algorithm, to solve it.

We demonstrate our framework with various 3D models of frame structures. Figure 1 shows one example of the bunny frame structure. We show the applications of the strengthening of weak parts and topology simplification while maintaining structural symmetry. Our results highlight the main concepts of the stress-oriented structural optimization.

2 Related Work

Fabrication-Aware Geometric Processing With the rapid development of techniques for 3D printing, many researchers have recently studied geometric processing problems for the purpose of fabrication. These fabrication-aware methods are typically led by a stress analysis that uses the finite element method. Stava et al. [5] introduce a method that deforms a model by hollowing, thickening and strut insertion. Zhou et al. [6] present a method to search for the worst-case stress under forces from all possible directions. Recently, a stochastic finite element method is used to compute failure probabilities [10] which can analyze the static soundness of one object. Prévost et al. [3] explore the problem of deforming shapes to make them physically balance.

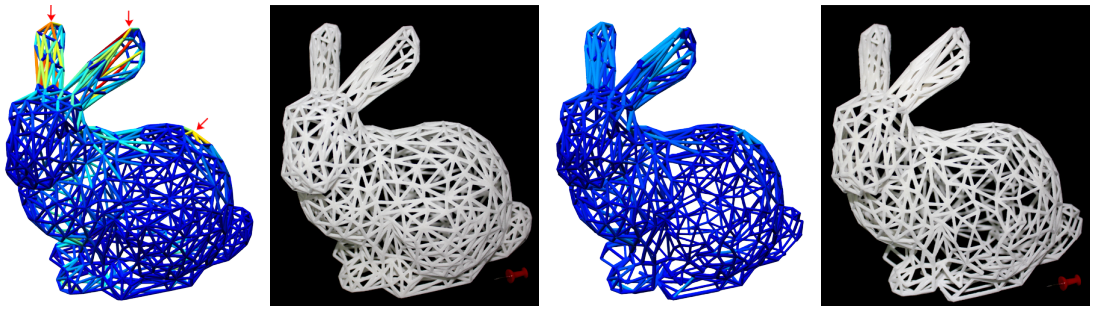

(a) (b) (c) (d)

Figure 1: Our approach analyzes an input 3D frame structure to perform simultaneous structural strengthening and simplification for 3D printing. (a) The input bunny frame model with 1569 beams. The external loads are denoted as red arrows. (b) A photo of the SLS 3D printed models of the input. A small red drawing pin is placed under the object as a size reference. (c) The resulting model obtained by our approach. The number of beams is reduced to 1319. (d) A photo of the SLS 3D printed models of our output.

Chen et al. [11] analyze elastic deformation caused by gravity to solve the inverse problem of computing a shape that when fabricated deforms naturally to a target shape. Yang et al. [12] design a support-free structure to print a balanced object without interior supports. Among this area of work, we contribute a stress-oriented problem formulation for automatically strengthening a frame structure while simplifying its structural complexity.

Structural Simplification for Fabrication There has been work on problems which aim to simplify the complexity of the structure of 3D shapes for fabrication. Many methods are based on decomposing a 3D shape into smaller pieces and then assembling them to form the original shape or a resemblance of it. Luo et al. [13] suggest a method to 3D print large objects by first segmenting an object into smaller parts and then assembling the parts to form the larger shape. Hildebrand et al. [14] create parts from a 3D shape that can then be fabricated and assembled in an optimal direction. Interlocked planar [15, 16] or solid pieces [17, 18] can be used to form a shape that resembles the original. Zimmer et al. [19] describe an approach to approximate mesh surfaces by building physical structures with the Zometool construction system. Vanek et al. [20] present a method to divide a mesh into parts which are then efficiently packed into space for 3D printing. Instead of decomposing a shape into smaller pieces, we simplify a frame structure by possibly removing elements from it. We contribute a semi-continuous optimization for this purpose.

Special Structure Design Motivated by existing architectural structures, some types of special 3D printed structures have been explored. Some structures, such as the skin-frame structure [8] and honeycomb-cells structure [9], are designed to reduce the cost of 3D printing via stress analysis. These methods are used for constructing the interior supporting structure of a solid object and these structures are cost-effective and are stable with high strength. Some structures are designed as the support structure necessary for 3D printing. The reduction of support structure can save printing time and material [21]. A bridge structure [4] can reduce the cost and meet stability conditions. Recently, Jiang et al. [22] propose a framework to generate a frame structure with different types of cross sections, which is statically sound and materially efficient. In this paper, we focus on strengthening and simplifying frame structures consisting of beams.

3 Preliminaries

This section describes the stress analysis and the representation of an input 3D shape of our algorithm as a frame structure. The stress computation described here is used in our optimization in Section 4.

3.1 Stress Computation

In continuum mechanics, stress is a physical quantity that expresses the internal forces that neighboring particles of a continuous material exert on each other [23, 24]. The strength of a material is measured in force per unit area, which depends on its capacity to withstand axial stress, shear stress, bending, and torsion. A static elastic object satisfies the following equilibrium equation:

$$\begin{cases} -\operatorname{div}\boldsymbol{\sigma}(\mathbf{u}) = \mathbf{f}, & \text{in } \Omega \\ \mathbf{u} = \mathbf{0}, & \text{on } \Gamma_H \\ \boldsymbol{\sigma}(\mathbf{u}) \cdot \mathbf{n} = \mathbf{g}, & \text{on } \Gamma_N \end{cases} \tag{1}$$

where $\mathbf{u}$ is the displacement, $\boldsymbol{\sigma}$ is the stress tensor, $\mathbf{f}$ is the body force, and $\mathbf{g}$ is the surface force. This differential equation is defined in the region of an object Ω, Γ_H and Γ_N are two open subsets of the boundary of Ω, such that

$\partial\Omega = \overline{\Gamma}_H \cup \overline{\Gamma}_N$ and $\Gamma_H \cap \Gamma_N = \emptyset$. We take the discretized form of this system, which becomes the linear equilibrium equation:

$$K\mathbf{u} = F \tag{2}$$

where K is the stiffness matrix and F is the external loads including body forces and surface forces.

3.2 Frame Structure

A frame structure consists of a set of beams and nodes where the beams are connected to each other at the nodes. Each beam is a cylindrical shape with a radius. The beams defines the topology (i.e. the connectivity between nodes) of the frame structure. According to theory on the frame structure [25, 26], the stiffness matrix K in Equation (2) can be computed for a frame structure, where K depends on the node positions and beam radii [8]. The forces in this equation are gravity or external loads we specify. We can then solve for the displacement and compute the stress for each beam in the frame structure. Although the stress is different in different part of the beam, we only consider the largest stress for each beam.

4 Problem and Formulation

We describe our problem formally in this section, including the objective function in our optimization, various constraints, and the problem formulation. The stress analysis from Section 3 allows us to compute the stress in our optimization. The solution to the optimization is presented in Section 5.

4.1 Problem

Stress Strengthening Our problem involves two components and the first component is structural strengthening. Structural optimization aims to determine the best design according to some objectives (e.g. greatest strength, maximum rigidity, lowest cost) under some constraints. A structure fails the strength criterion when the stress (force divided by area of material) induced by the load is greater than the capacity of the structural material to resist the load without breaking, or when the strain (percentage extension) is so great that the element no longer fulfills its function. As acknowledged in the literature [27, 28, 29], it is natural to use stress or strain as criteria for the weakness measure of a target structure. Hence we use stress as a criterion for the purpose of structural strengthening.

Structural Complexity The second motivation is complexity. There exists many beams in our frame structures and some of these beams are not significant to the stress of the overall structure. We may therefore remove some of them without affecting the stress of the overall shape and to simplify its structural complexity.

Problem The input to our problem is a frame structure of beams. Considering the above two components, our problem is to perform simultaneous stress strengthening and structural complexity reduction of the input shape under some external loads. The output is a modified frame structure with a smaller number of beams while the stress of the shape is maintained or strengthened. The radii of some beams are adjusted while some beams are removed. The resulting shape may be 3D printed as a structure with high strength and simplified complexity.

4.2 Objective Function

Objective Function Let $\mathcal{M}$ be a mesh representing the frame structure. We adopt stress as a criterion for the weakness measure of an object and minimize the maximal stress of the beams in the structure. The stress-oriented structural optimization problem can thus be formulated as

$$\mathbf{s}^* = \arg\min_{\mathbf{s}\in\Theta} \max_{\mathbf{p}\in\mathcal{M}(\mathbf{s})} \sigma(\mathbf{p}) \tag{3}$$

where $\mathbf{s}$ is the vector of structural design variables, Θ is the collection of all feasible design variables, and θ is the stress function. The solution of the above problem is $\mathbf{s}^*$, and $\mathcal{M}(\mathbf{s}^*)$ is then the output shape.

Design Variables The degree of freedom of the structural design space is large in general. Hence we simplify the problem by focusing on a piecewise scaling transformation for each element of the shape. Let $\mathcal{K} = (V_\mathcal{K}, E_\mathcal{K})$ be the frame structure of a shape, where $V_\mathcal{K}$ and $E_\mathcal{K}$ represent the set of nodes and beams respectively. For every beam, we define a scalar s_i, $i \in \{1, \cdots, |E_\mathcal{K}|\}$ which is the scaling factor of the radius of each beam. Let $\mathbf{s} = (s_1, s_2, \cdots, s_{|E_\mathcal{K}|})$ be our set of structural design variables. We can perform many changes to the shape by adjusting these scalar variables. For example, we can adjust s_i to strengthen weak parts. We can re-distribute volume in the overall shape by adjusting s_i for multiple parts. If we set $\mathbf{s}_o = \mathbf{1} = (1, 1, \cdots, 1)$, then $\mathcal{M}(\mathbf{s}_o)$ is the original object. If we set some $s_i = 0$ then the corresponding part will disappear and we can perform topological changes to the overall shape.

4.3 Constraints

We consider various constraints in our framework to maintain the size, aesthetics, and complexity of the output shape.

Volume Constraint We compute the shape's volume by adding the volume of all beams. Each beam's volume is estimated as the cross sectional area multiplied by its length. We can write the volume constraint as:

$$\mathrm{Vol}(\mathbf{s}) \leq \gamma\,\mathrm{Vol}(\mathbf{1}) \tag{4}$$

where γ is a user-specified value which means that the resulting volume is no more than γ of the original volume.

Symmetry Constraint In many practical applications, it is important to maintain the symmetry of a shape during its structural optimization, so as to maintain its overall aesthetics. Our approach can achieve this by adding symmetry constraints as follows:

$$s_i - s_j = 0,\ (i,j) \in \mathcal{S} \tag{5}$$

where $\mathcal{S}$ is the set of index pairs of beams that we wish to maintain symmetry with.

Semi-continuous Constraint In order to satisfy the printability of the object, the scalar s_i should be within an interval $[a_i, b_i]$. For example, the scalar should be set such that the thickness of the shape is not less than the minimum manufacturable size of the 3D printer. Each scalar s_i can also take a zero value. Hence this leads to a semi-continuous condition:

$$s_i \in [a_i, b_i] \cup \{0\}, \quad i \in \mathcal{I} = \{1, 2, \cdots, |E_{\mathcal{K}}|\}. \tag{6}$$

Sparsity Constraint Moreover, we can add a cardinality constraint to control the overall complexity of the structure:

$$\|\mathbf{s}\|_0 \leq \tau. \tag{7}$$

4.4 Formulation

We can now formulate our stress-oriented structural optimization as follows

$$\begin{aligned} \arg\min_{\mathbf{s}} \quad & \max_{e \in \mathcal{E}} \sigma_e(\mathbf{s}) \\ \text{s.t.} \quad & \mathrm{Vol}(\mathbf{s}) \leq \gamma\, \mathrm{Vol}(\mathbf{1}) \\ & s_i - s_j = 0,\ (i,j) \in \mathcal{S} \\ & s_i \in [a_i, b_i] \cup \{0\},\ i \in \mathcal{I} \\ & \|\mathbf{s}\|_0 \leq \tau \end{aligned} \tag{8}$$

where $\mathcal{E}$ is the set of beams in the frame structure, and σ_e is the stress function described in the previous section.

5 Semi-Continuous Optimization

In the formulation of our optimization (Equation (8)), the scaling factors $\mathbf{s}$ are a set of semi-continuous decision variables [30, 31]. Theoretically, it is in general NP-hard to solve this kind of highly nonlinear optimization problem which has combinatorial nature (semi-continuous sparsity) [32, 33]. Thus we reformulate our problem and then mathematically derive an algorithm based on the ADMM (alternating direction method of multipliers) strategy [34, 35] to solve it. The ADMM method is designed to solve convex optimization problems by breaking them into smaller pieces, and it has been applied to a number of problems arising in statistics and machine learning [35, 36]. The semi-continuous condition in our problem formulation leads to two sets of variables. The idea of ADMM is to split the optimization into sub-problems that iteratively find solutions to the two sets of variables.

5.1 Problem Reformulation

We add a new variable δ to represent the maximum stress and introduce a variable splitting strategy (and a new variable $\mathbf{y}$) to reformulate the problem in Equation (8) as:

$$\begin{aligned} \arg\min_{(\mathbf{s},\delta,\mathbf{y})} \quad & \delta \\ \text{s.t.} \quad & \sigma_e(\mathbf{s}) - \delta \leq 0,\ e \in \mathcal{E} \\ & \mathrm{Vol}(\mathbf{s}) \leq \gamma\, \mathrm{Vol}(\mathbf{1}) \\ & s_i - s_j = 0,\ (i,j) \in \mathcal{S} \\ & \mathbf{s} - \mathbf{y} = 0 \\ & \mathbf{y} \in \mathcal{Y} \end{aligned} \tag{9}$$

where $\mathcal{Y} = \{\mathbf{y} \mid a_i z_i \leq y_i \leq b_i z_i, z_i \in \{0,1\}, i \in \mathcal{I}; \mathbf{1}^T \mathbf{z} \leq \tau\}$. The optimal $\mathbf{s}^*$ is our solution. The advantage of introducing the variable $\mathbf{y}$ is that it allows the decoupling of the continuous constraint and the semi-continuous sparsity constraint, since each of them now applies to one specific optimization variable $\mathbf{s}$ or $\mathbf{y}$. Although we introduce an additional constraint, it is now easier to solve the reformulated problem (Equation (9)) than the original one (Equation (8))

5.2 Solution

Our solution is based on ADMM which is itself based on an augmented Lagrangian function and two sub-problems within the overall optimization. We describe these in detail in this sub-section.

Augmented Lagrangian One typical way for solving such an optimization problem is to use an augmented Lagrangian approach [37]. We use this method and define the problem's augmented Lagrangian function as follows:

$$L_\rho(\mathbf{s}, \delta, \mathbf{y}, \boldsymbol{\lambda}) = \delta + \boldsymbol{\lambda}^T(\mathbf{s} - \mathbf{y}) + \frac{\rho}{2}\|\mathbf{s} - \mathbf{y}\|^2 \tag{10}$$

with $\boldsymbol{\lambda}$ being the Lagrangian multipliers and ρ a positive parameter that balances the quadratic penalization.

Pseudocode Instead of a joint optimization on the two variables, the idea of ADMM is to optimize alternatively over $(\mathbf{s}, \delta)$ and $\mathbf{y}$. Algorithm 1 gives the pseudocode of our solution with ADMM. The stopping criterion in the optimization is: the value of the function has almost no change or the number of iteration steps reaches a given upper bound.

$(\mathbf{s}, \delta)$-subproblem The $(\mathbf{s}, \delta)$-subproblem in the ADMM algorithm involves a quadratic objective and the continuous constraint. We use the interior-point method to solve the subproblem:

$$\min_{(\mathbf{s},\delta) \in \mathcal{D}} \delta + \frac{\rho}{2}\|\mathbf{s} - (\mathbf{y}^k - \boldsymbol{\lambda}^k/\rho)\|^2 \tag{11}$$

where $\mathcal{D} = \{(\mathbf{s}, \delta) \mid \sigma_e(\mathbf{s}) - \delta \leq 0, e \in \mathcal{E}; \mathrm{Vol}(\mathbf{s}) \leq \gamma\, \mathrm{Vol}(\mathbf{1}); s_i - s_j = 0, (i,j) \in \mathcal{S}\}$ is the feasible set of continuous variables.

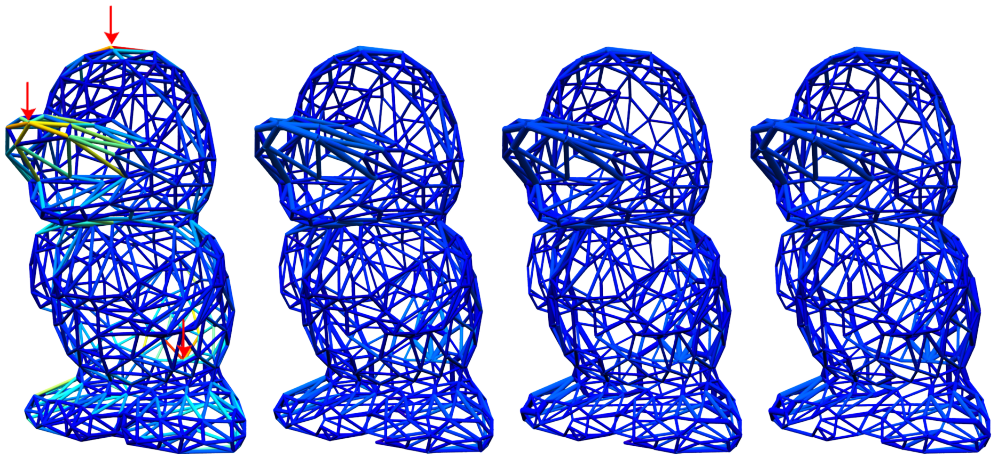

(a) (b) (c) (d)

Figure 2: The results of applying our approach on a frame structure of a duck. (a) The input duck model with 1107 beams. Three external loads (marked as red arrows) are applied on the model. (b,c,d) The simplified duck models (with 1007, 957, 907 beams respectively) obtained with our approach. The resulting models are increasingly simplified while their structures still remain strong.

Algorithm 1 The ADMM algorithm for structural optimization

Input: an initial structure $\mathcal{M}(\mathbf{s}^o)$

Step 0: Set $k = 0$ and initialize $\mathbf{y}^0, \boldsymbol{\lambda}^0$. Set the penalty parameter ρ and the step-size α.

Repeat

Step 1: Solve the $(\mathbf{s}, \delta)$-subproblem

$$(\mathbf{s}^{k+1}, \delta^{k+1}) = \arg\min_{(\mathbf{s},\delta)\in\mathcal{D}} L_\rho(\mathbf{s}, \delta, \mathbf{y}^k, \boldsymbol{\lambda}^k)$$

Step 2: Solve the $\mathbf{y}$-subproblem

$$\mathbf{y}^{k+1} = \arg\min_{\mathbf{y}\in\mathcal{Y}} L_\rho(\mathbf{s}^{k+1}, \delta^{k+1}, \mathbf{y}, \boldsymbol{\lambda}^k)$$

Step 3: Update the Lagrangian multipliers

$$\boldsymbol{\lambda}^{k+1} = \boldsymbol{\lambda}^k + \alpha\rho(\mathbf{s}^{k+1} - \mathbf{y}^{k+1})$$

Until stopping criterion is met.

Output: an optimized structure $\mathcal{M}(\mathbf{s}^*)$ with its optimal variable $\mathbf{s}$

$\mathbf{y}$-subproblem We rewrite the $\mathbf{y}$-subproblem as a close-form solution, starting with:

$$\min_{\mathbf{y}\in\mathcal{Y}} \quad \|\mathbf{y} - (\mathbf{s}^{k+1} + \boldsymbol{\lambda}^k/\rho)\|^2 = \sum_i (y_i - t_i)^2 \tag{12}$$

with $t_i = s_i^{k+1} + \lambda_i^k/\rho$. If $y_i \neq 0$, we denote

$$\zeta_i = \min_{\mathbf{y}\in\mathcal{Y}} (y_i - t_i)^2 = \begin{cases} (a_i - t_i)^2 & t_i < a_i, \\ 0 & a_i \le t_i \le b_i, \\ (b_i - t_i)^2 & t_i > b_i. \end{cases}$$

Then this subproblem can be further simplified as:

$$\begin{aligned} \min_{\mathbf{z}} \quad & \sum_i \left[t_i^2(1 - z_i) + \zeta_i z_i\right] = \sum_i t_i^2 - \sum_i (t_i^2 - \zeta_i) z_i \\ \text{s.t.} \quad & z_i \in \{0, 1\}, i \in \mathcal{I};\ \mathbf{1}^T\mathbf{z} \le \tau. \end{aligned} \tag{13}$$

Let $\{t_{\ell_1}^2 - \zeta_{\ell_1}, t_{\ell_2}^2 - \zeta_{\ell_2}, \cdots, t_{\ell_\tau}^2 - \zeta_{\ell_\tau}\}$ be the first τ positive numbers of sequence $\{t_i^2 - \zeta_i\}_{i\in\mathcal{I}}$ in descending order. The problem in Equation (13) has the solution $z_{\ell_1} = z_{\ell_2} = \cdots = z_{\ell_\tau} = 1;\ z_i = 0, i \notin \{\ell_1, \ell_2, \cdots, \ell_\tau\}$. Finally, we get a closed-form solution

$$y_i = \max(a_i, \min(t_i, b_i)) \cdot z_i \quad \forall i \in \mathcal{I}$$

for the $\mathbf{y}$-subproblem (Equation (12)).

6 Experimental Results

We have implemented our algorithm and tested it on various models. All the examples presented in this paper were created with a dual-core 3.5 GHz machine with 8G memory. We have 3D printed some of the models to demonstrate our results.

There are several parameters in our formulation. The user can change the value of the weight γ to control the volume of the resulting object. We set $\gamma = 1$ in our implementation which means that we do not want to increase the volume of the result adjusting the shape. Another parameter is τ which measures the complexity of the structure by measuring the number of beams. Thus τ can be adjusted by the user and set to a number less than the total number of beams in the input model. We specify the external loads manually at various points of the input shapes. In the optimization, we set the penalty parameter ρ to be 10 and the step-size α to be 0.6.

(a) (b) (c) (d) (e) (f)

Figure 3: Results of applying our approach on the eiffel tower model. (a) The input Eiffel Tower frame model with 1521 beams. (b) The computed stress of the input model under an external load of 2N (shown by red arrow). (c) A photo of the SLS 3D printed model of the input. A small red pin is placed under the object as a size reference. (d) The simplified frame model with 1341 beams obtained by our approach. (e) The computed stress of the output model under the same external load as that of the input in (b). We can see that the output model has higher strength and reduced complexity. (f) The photo of the SLS 3D printed model of our output.

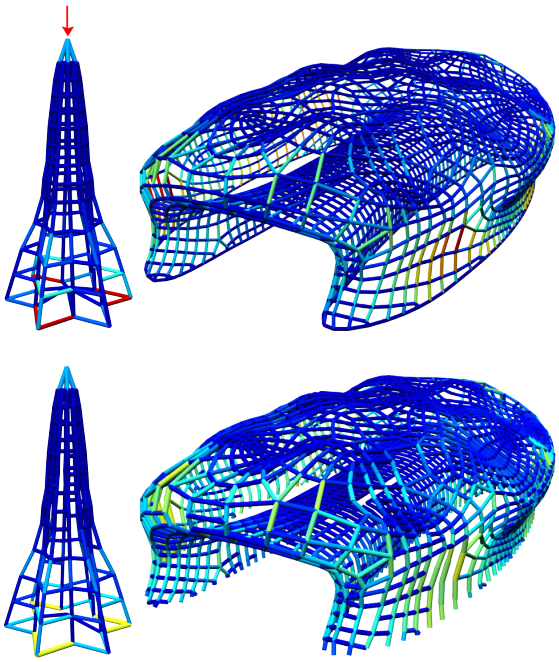

Figure 4: Results of applying our approach on the boomerang model (left) and the airport model (right). An external load (shown in red arrow) is applied on the boomerang model. Gravity is applied as external load to the airport model. The original models (top) have 312 and 5045 beams respectively. Our results (bottom) have 284 and 4585 beams respectively and they are both structurally simplified and strengthened compared to the originals.

Figure 2 shows the results of our algorithm on a frame structure of a duck model. We set different values of the sparsity parameter τ and obtain a sequence of results. The resulting structural shapes in Figure 2(b,c,d) are progressively simplified in the number of beams while their strengths are maintained.

Figure 3 shows an example of eiffel tower. In this example, since the feet of the tower are fixed, the beams connecting fixed nodes have zero stress, thereby being removed.

Figure 4 shows two examples whose external loads are vertical down. The left one is the frame structure of boomerang. Since the given external force is vertical down, some horizontal beams have less contribution to the soundness, thus being removed by our optimization. The right one is the airport model with a constant gravity on each node. Note that there are also some horizontal beams removed due to the similar reason.

Figure 5 show the result of a complicated structure. The model demonstrate the application of our method to both structural simplification and strengthening, as the results have reduced complexity and higher structural strength.

7 Conclusion

We present a novel approach for performing structural analysis on 3D shapes with simultaneous structural strengthening and simplification. The optimized shape can be 3D printed with high strength and reduced complexity. We use stress as a criterion for measuring strength and minimize the maximal stress of the shape to formulate an optimization with a semi-

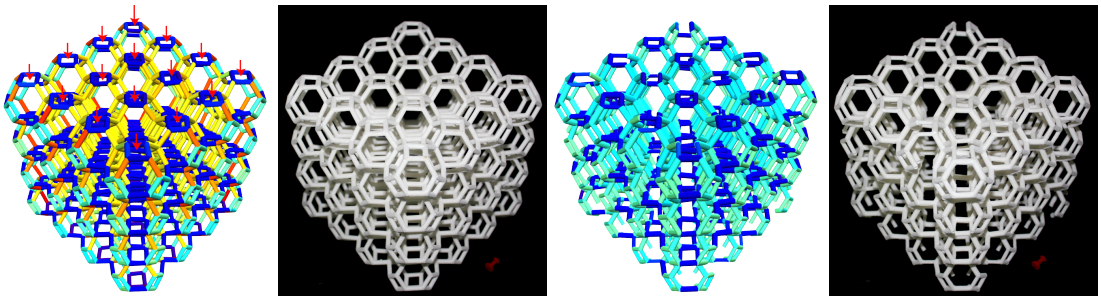

(a) (b) (c) (d)

Figure 5: Results of applying our approach on the "hardstruct" model. (a) The input model where external loads are denoted as red arrows. The hardstruct model has 1728 beams. (b) We 3D printed the input model with a Sinterstation SLS 3D printer. A small red pin is placed under the object as a size reference. (c) The resulting model obtained by our approach is structurally simplified and strengthened with our approach. The hardstruct model has 1548 beams. (d) We physically demonstrate our results by 3D printing the output model.

continuous condition. We then derive an algorithm based on the ADMM method to solve the optimization and show its applicability and feasibility towards topology simplification and structural strengthening. Although this paper focuses on frame structures, our framework can be extended to general meshes by considering them as skeletal tetrahedral structures and we leave this for future work.

One limitation of our work is that we do not move the positions of the nodes in a structure. This means that although the structure can be much simplified, the inherent topology of the original structure remains the same. Moving the positions of the nodes can potentially be done in our optimization framework. However, this will enlarge the dimensions of the variable space and will need higher computational cost. We leave this as a future research direction.

Another area of future work that is relevant for fabrication is the computation of supporting structures for FDM 3D printing. There has already been previous work in this area recently. Applying our stress-oriented structural optimization to this problem would be an interesting direction.

References

[1] Bernd Bickel, Moritz Bächer, Miguel A. Otaduy, Hyunho Richard Lee, Hanspeter Pfister, Markus Gross, and Wojciech Matusik. Design and fabrication of materials with desired deformation behavior. *ACM Transactions on Graphics*, 29(4):63:1–63:10, July 2010.

[2] Stelian Coros, Bernhard Thomaszewski, Gioacchino Noris, Shinjiro Sueda, Moira Forberg, Robert W. Sumner, Wojciech Matusik, and Bernd Bickel. Computational design of mechanical characters. *ACM Transactions on Graphics*, 32(4):83:1–83:12, July 2013.

[3] Romain Prévost, Emily Whiting, Sylvain Lefebvre, and Olga Sorkine-Hornung. Make it stand: Balancing shapes for 3D fabrication. *ACM Transactions on Graphics*, 32(4):81, 2013.

[4] Jérémie Dumas, Jean Hergel, and Sylvain Lefebvre. Bridging the gap: Automated steady scaffoldings for 3D printing. *ACM Transactions on Graphics*, 33(4):98, 2014.

[5] Ondrej Stava, Juraj Vanek, Bedrich Benes, Nathan Carr, and Radomír Měch. Stress Relief: Improving structural strength of 3D printable objects. *ACM Transactions on Graphics*, 31(4):48, 2012.

[6] Qingnan Zhou, Julian Panetta, and Denis Zorin. Worst-case structural analysis. *ACM Transactions on Graphics*, 32(4):137, 2013.

[7] Yue Xie, Weiwei Xu, Yin Yang, Xiaohu Guo, and Kun Zhou. Agile structural analysis for fabrication-aware shape editing. *Computer Aided Geometric Design*, 35-36(5):163C179, 2015.

[8] Weiming Wang, Tuanfeng Y Wang, Zhouwang Yang, Ligang Liu, Xin Tong, Weihua Tong, Jiansong Deng, Falai Chen, and Xiuping Liu. Cost-effective printing of 3D objects with skin-frame structures. *ACM Transactions on Graphics*, 32(6):177, 2013.

[9] Lin Lu, Andrei Sharf, Haisen Zhao, Yuan Wei, Qingnan Fan, Xuelin Chen, Yann Savoye, Changhe Tu, Daniel Cohen-Or, and Baoquan Chen. Build-to-last: Strength to weight 3D printed objects. *ACM Transactions on Graphics*, 33(4):97, 2014.

[10] Timothy Langlois, Ariel Shamir, Daniel Dror, Wojciech Matusik, and David IW Levin. Stochastic structural analysis for context-aware design and fabrication. *ACM Transactions on Graphics (TOG)*, 35(6):226, 2016.

[11] Xiang Chen, Changxi Zheng, Weiwei Xu, and Kun Zhou. An asymptotic numerical method for inverse elastic shape design. *ACM Transactions on Graphics*, 33(4):95, 2014.

[12] Yang Yang, Shuangming Chai, and Xiao-Ming Fu. Computing interior support-free structure via hollow-to-fill construction. *Computers & Graphics*, 2017.

[13] Linjie Luo, Ilya Baran, Szymon Rusinkiewicz, and Wojciech Matusik. Chopper: Partitioning models into 3d-printable parts. *ACM Transactions on Graphics*, 31(6):129, 2012.

[14] Kristian Hildebrand, Bernd Bickel, and Marc Alexa. Orthogonal slicing for additive manufacturing. *Shape Modeling International (SMI)*, 37(6):669–675, 2013.

[15] Yuliy Schwartzburg and Mark Pauly. Fabrication-aware design with intersecting planar pieces. *Computer Graphics Forum*, 2013.

[16] Paolo Cignoni, Nico Pietroni, Luigi Malomo, and Roberto Scopigno. Field-aligned mesh joinery. *ACM Transactions on Graphics*, 33(1):11:1–11:12, 2014.

[17] Peng Song, Chi-Wing Fu, and Daniel Cohen-Or. Recursive interlocking puzzles. *ACM Transactions on Graphics (SIGGRAPH Asia)*, 31(6), 2012. Article 128.

[18] Peng Song, Zhongqi Fu, Ligang Liu, and Chi-Wing Fu. Printing 3d objects with interlocking parts. *Computer Aided Geometric design (Proc. of GMP 2015)*, 35-36(5):137C148, 2015.

[19] Henrik Zimmer, Florent Lafarge, Pierre Alliez, and Leif Kobbelt. Zometool shape approximation. *Graphical Models*, 76(5):390–401, 2014.

[20] J. Vanek, J. A. Garcia Galicia, B. Benes, R. Měch, N. Carr, O. Stava, and G. S. Miller. Packmerger: A 3d print volume optimizer. *Computer Graphics Forum*, 33(6):322–332, 2014.

[21] J. Vanek, J. A. Garcia Galicia, and B. Benes. Clever support: Efficient support structure generation for digital fabrication. *Computer Graphics Forum*, 33(5):117–125, 2014.

[22] Caigui Jiang, Chengcheng Tang, Hans-Peter Seidel, and Peter Wonka. Design and volume optimization of space structures. *ACM Transactions on Graphics (TOG)*, 36(4):159, 2017.

[23] Lev D Landau and E. M. Lifshitz. *Theory of Elasticity*. Course of Theoretical Physics 3. Elsevier, 1986.

[24] Mohammed Ameen. *Computational Elasticity: Theory of Elasticity and Finite and Boundary Element Methods*. Alpha Science Int'l Ltd., 2005.

[25] Thomas JR Hughes. *The finite element method: linear static and dynamic finite element analysis*. Courier Corporation, 2012.

[26] Lorna J Gibson and Michael F Ashby. *Cellular solids: structure and properties*. Cambridge university press, 1999.

[27] Clive L Dym. *Structural Modeling and Analysis*. Cambridge University Press, 1997.

[28] Jacques Heyman. *The Science of Structural Engineering*. Imperial College Press, London, UK, 1999.

[29] Keith D Hjelmstad. *Fundamentals of Structural Mechanics*. Springer Science & Business Media, Inc, 2007.

[30] I. de Farias and M. Zhao. A polyhedral study of the semi-continuous knapsack problem. *Mathematical Programming*, 142(1-2):169–203, 2013.

[31] X. Sun, X. Zheng, and D. Li. Recent advances in mathematical programming with semi-continuous variables and cardinality constraint. *Journal of the Operations Research Society of China*, 1(1):55–77, 2013.

[32] D. Bienstock. Computational study of a family of mixed-integer quadratic programming problems. *Mathematical Programming*, 74(2):121–140, 1996.

[33] G. Fung and O. Mangasarian. Equivalence of minimal l(0)- and l(p)-norm solutions of linear equalities, inequalities and linear programs for sufficiently small p. *Journal of Optimization Theory and Applications*, 151(1):1–10, 2011.

[34] J. Eckstein and D. P. Bertsekas. On the Douglas-Rachford splitting method and the proximal point algorithm for maximal monotone operators. *Mathematical Programming*, 55(1-3):293–318, 1992.

[35] S. Boyd, N. Parikh, E. Chu, B. Peleato, and J. Eckstein. Distributed optimization and statistical learning via the alternating direction method of multipliers. *Foundations and Trends in Machine Learning*, 3(1):1–122, 2011.

[36] E. Chu, A. Keshavarz, and S. Boyd. A distributed algorithm for fitting generalized additive models. *Optimization and Engineering*, 14(2):213–224, 2013.

[37] J. Nocedal and S.J. Wright. *Numerical Optimization*. Series in Operations Research and Financial Engineering. Springer, 2006.